

# Innovative Approaches to Enhancing Oocyte Competence in patients with polycystic ovarian syndrome: A Microfluidic Study with the Impact of FF-MAS on Rescued In Vitro Oocyte Maturation

Hossein torkashvand

Iran University of Medical Sciences

Ronak Shabani

Iran University of Medical Sciences

Tayebe Artimani

Hamedan University of Medical Sciences

Shamim Pilehvari

Hamedan University of Medical Sciences

Mahdi Moghimi

Iran University of Science and Technology

mehdi mehdizadeh

Mehdizadeh.m@iums.ac.ir

Iran University of Medical Sciences

---

## Article

**Keywords:** Assisted Reproductive Technology (ART), In vitro Maturation (IVM), Oocyte, Microfluidic Chip, Follicular fluid meiosis-activating sterol (FF-MAS)

**Posted Date:** April 30th, 2024

**DOI:** <https://doi.org/10.21203/rs.3.rs-4188416/v1>

**License:** © ⓘ This work is licensed under a Creative Commons Attribution 4.0 International License.

[Read Full License](#)

**Additional Declarations:** No competing interests reported.

---

# Abstract

Polycystic ovary syndrome (PCOS), a common endocrine disorder in reproductive-age women, often results in infertility due to anovulation, increased immature oocytes, and reduced oocyte quality. Assisted Reproductive Technology (ART), specifically in vitro maturation (IVM), offers potential solutions. This study explores in vitro oocyte maturation using a novel microfluidic device. We investigate the impact of Follicular fluid meiosis-activating sterol (FF-MAS) under dynamic and static conditions to enhance oocyte competence. 406 immature germinal vesicle (GV) oocytes from PCOS patients were divided into five groups. Group 1: GV oocytes cultured in standard medium. Group 2: same as Group 1 In addition 10  $\mu$ M FF-MAS supplement. Group 3 experienced dynamic microfluidic culture for 24 hours. Groups 4 and 5 also utilized dynamic microfluidic culture, but in Group 4, FF-MAS was provided to the oocytes for the first 2 hours, and in Group 5, it was provided for the entire 24 h. Groups 4 and 5 showed significantly improved maturation, fertilization, and high-quality embryo development. Gene expression analysis revealed differences in BRCA1, TP53, PADI6, and TLE6 genes. Ultrastructural features indicated cortical granule distribution and cytoplasmic observations in mature oocytes. Dynamic microfluidic culture and FF-MAS supplementation enhance developmental competency compared to static conditions.

## Introduction

Polycystic ovary syndrome (PCOS) is a prevalent endocrine disorder impacting 5–10% of women in their reproductive age, causing infertility <sup>1,2</sup>. While the exact cause of PCOS remains uncertain, it is characterized by symptoms such as hyperandrogenism, chronic anovulation, and the presence of numerous small cysts on the ovaries <sup>3</sup>. In individuals with PCOS, chronic anovulation and other factors, including an increase in immature oocytes and a decrease in oocyte quality, fertilization, and implantation rates, contribute to infertility <sup>4</sup>. Thus, the use of Assisted Reproductive Technology (ART) can potentially enhance oocyte competence and aid in selecting embryos of the highest quality for transfer.

The path to understanding and mitigating the challenges posed by PCOS involves exploring innovative approaches in the field of ART. In vitro maturation (IVM) of immature oocytes obtained from PCOS patients presents a promising strategy to reduce the associated costs and clinical complications often linked with In Vitro Fertilization (IVF) <sup>5</sup>. While the birth of healthy infants has been reported after IVM procedures, but the pregnancy rates are notably lower compared to oocytes matured in vivo or using other methods. Therefore, enhancing the success rate of IVM continues to be a critical challenge in improving efficiency for fertility preservation <sup>6</sup>.

Amidst the myriad of substances that have been reported to affect oocyte maturation, lies a promising endogenous signaling molecule: FF-MAS (4,4-dimethyl-5 $\alpha$ -cholest-8,14,24-trien-3 $\beta$ -ol). This molecule serves as an intermediary in the cholesterol biosynthetic pathway, found within all cell types <sup>7</sup>. Follicular fluid meiosis-activating sterol (FF-MAS), a sterol from human follicular fluid, was proven to be

stimulatory to resumption of meiosis in human oocytes<sup>8</sup>. FF-MAS, exhibits a notable increase in concentration within the preovulatory follicle during the process of oocyte maturation. During ovulation, the oocyte is released along with the follicular fluid, suggesting continued exposure to MAS during the first part of its passage through the oviduct. However, during IVM or IVF, when oocytes are retrieved and placed in a controlled environment, they lack direct contact with FF-MAS. This absence of exposure potentially impacts oocyte maturation, particularly in patients with PCOS who commonly exhibit deficiencies in oocyte meiosis development<sup>9,10</sup>.

On the other hand, within the in vivo setting, ovulated oocytes before fertilization are restricted within the female reproductive tract, enclosed in a limited amount of oviductal or uterine fluid. Conversely, the in vitro situation presents a stark contrast. In vitro, both oocytes and embryos undergo cultivation in a notably larger volume of culture medium<sup>11</sup>. In order to elevate oocyte competence and perfect the in vitro maturation process, it is imperative that static oocyte culturing systems undergo a transformation to more faithfully emulate the dynamic environment of the mammalian female reproductive tract, more accurately replicating the natural conditions of the ovary and fallopian tube<sup>12</sup>. Significant distinctions exist when comparing static (conventional) culture conditions to the dynamic conditions of the in vivo environment<sup>13,14</sup>. What can effectively address this challenge is the advancement of modern microfluidics technology through device miniaturization or the establishment of a dynamic environment, often referred to as lab-on-a-chip (LOC)<sup>15</sup>. Despite many attempts to develop tools effective in the maturation of oocytes and the culture of embryos, dynamic microfluidic devices have not yet been widely adopted in clinical embryology laboratories<sup>16</sup>. Microfluidic systems offer a more physiologically relevant environment, potentially enhancing oocyte maturation efficiency and facilitating subsequent embryo development<sup>17</sup>. By simulating the natural maturation process, these microfluidic methods represent a significant stride toward optimizing assisted reproductive technologies for improved outcomes in fertility treatments<sup>18</sup>.

In this study, our investigation centers on the design and fabrication of an innovative microfluidic device. Beyond assessing the impact of a microfluidic culture system on the maturation of immature oocytes with precise timing, our research focuses on evaluating the influence of the FF-MAS factor on the maturation rate of immature oocytes under dynamic conditions. Additionally, we conduct a comparative analysis, examining the maturation rate of immature oocytes in static conditions. Our objective is to replicate the natural conditions of the ovary and fallopian tube, with the aim of optimizing the in vitro maturation process and enhancing oocyte competence. Ultimately, our goal is to improve outcomes in assisted reproductive technologies for individuals with PCOS.

## Material and method

### 2.1 Ethical approval

All methods were carried out in accordance with relevant guidelines and regulations. The study received approval from the ethics committee of Iran University of Medical Sciences in Tehran, Iran (IR.IUMS.FMD.REC.1401.314). Written consent was acquired from all participants involved in this research.

## **2-2 Patients selection**

The research was carried out at the Infertility Center of Fatemieh Hospital in Hamedan, spanning from November 2021 to August 2023. A total of 438 GV oocytes were obtained from 163 patients with PCOS referred to the Infertility Center. Patients were selected based on the Rotterdam criteria<sup>19</sup>. The age range and body mass index (BMI) were 20–35 years and 20–27 kg/m<sup>2</sup>, respectively, with no male factor infertility (total volume > 1.5 cc, concentration > 15 million/ml, total motility > 40%, and normal morphology > 4%, according to the WHO 2010 criteria). Uterine disorders, diabetes background, endometriosis background, as well as endocrine and inflammatory disorders, including congenital adrenal hyperplasia, Cushing's syndrome, hyperprolactinemia, and thyroid gland diseases, were considered as exclusion criteria. The inclusion criteria for oocytes were limited to those that were morphologically normal. Oocytes with cytoplasmic or extra cytoplasmic abnormalities, such as irregular shape, dark cytoplasm, diffuse granulation, perivitelline space, central cytoplasmic granulation, or oocytes at stage of MI, were excluded from the study.

## **2-3 Ovarian stimulation protocol**

The patients underwent controlled ovarian stimulation, according to gonadotropin-releasing hormone (GnRH) antagonist protocol. Prior to the onset of menstruation, the patients received a daily dose of 4 mg of estradiol valerate for a duration of 10 days. The stimulation was initiated using recombinant follicle-stimulating hormone (rFSH: Gonal-F® by Merck, Geneva, Switzerland) at a dose of 150 IU on day 2 or 3 of the menstrual cycle. When the largest follicle reached a size of 14 mm, GnRH antagonist (Cetrotide, Merck Serono, Germany) was administered via subcutaneous injection (0.25 mg/day), and continued until the oocyte trigger was administered. Daily monitoring of follicle growth was conducted through transvaginal sonography. We induced ovulation by administering a 0.2 mg GnRH agonist decapeptide (Ferring, Copenhagen NV) when at least two follicles reached a size of 18–20 mm. Subsequently, the ovum pickup was scheduled 36 hours later, under the guidance of vaginal ultrasound. Importantly, we did not encounter any instances of ovarian hyperstimulation syndrome<sup>20</sup>.

## **2-4 Retrieval of immature oocytes**

After aspiration, the cumulus-oocyte complexes (COCs) were carefully extracted from the collection fluid using a sterile pipette. Afterward, they were placed in a culture medium (G-IVF; Vitrolife, Kungsbacka, Sweden), covered with paraffin oil (MediCult), and incubated at 37 °C with 6% CO<sub>2</sub> for a duration of 3 hours. The cumulus cells (CCs) were efficiently removed enzymatically using 80 IU/mL of hyaluronidase (Sigma, St. Louis, MO, USA) and mechanical manipulation with glass pipettes. Following denudation, the oocytes are carefully washed in G-Mops-V1 (Vitrolife) and subsequently transferred to a petri dish

containing culture medium. Then, they are meticulously classified into germinal vesicle (GV), metaphase I (MI), or Metaphase II (MII) stages based on their respective meiotic maturation stage under a stereomicroscope (Olympus Co., Tokyo, Japan).

## **2-5 Preparation meiosis activating sterol (FF-MAS)**

FF-MAS was purified from human follicular fluid using Byskov's laboratory procedure <sup>21</sup>. Briefly, 1 ml of follicular fluid (FF) was mixed with a 75% n-heptane and 25% isopropanol solution. Subsequently, 0.1 ml of 0.3 M NaH<sub>2</sub>PO<sub>4</sub> (pH 1.0) was added, which was vigorously shaken for 2 hours. The resulting solution was then centrifuged for 10 minutes at 2000 rpm to separate the organic phase containing sterols. This phase was collected, dried, and flushed with 2 ml of n-heptane, followed by centrifugation for 5 minutes at 2000 rpm. Supernatants obtained were dried and reconstituted in 150 µg of HPLC eluent. These reconstituted samples were subsequently loaded onto a straight-phase HPLC column (ChromspherSi, 5 µm, 250 mm × 4.6 mm) using a mixture of 99.5% n-heptane and 0.5% isopropanol (v:v), running at a flow rate of 1.00 ml/min. Specific sterols (lanosterol and T-MAS) were collected from the HPLC column. Reversed-phase separation was conducted by reconstituting the collected samples in acetonitrile and loading them onto a LiChrospher RP-8, 5 µm, 150 mm × 3.0 mm HPLC column. This column was run with a mobile phase consisting of 93% acetonitrile and 7% water (v/v) at a flow rate of 1.00 ml/min and at room temperature. Quantification was done by comparing the eluted peaks from the samples with runs of standards (lanosterol, cholesterol, FF-MAS, and T-MAS) using known concentrations of these standards.

## **2-6 Microfluidic chip**

The design principles behind this microfluidic device are grounded in simulating the natural growth conditions of the oocyte and embryo *in vivo* <sup>22</sup>. The device was manufactured at the Mizan Microchip Technology Laboratory in Tehran, Iran. Utilizing CAD (AutoCAD) software, the 3D geometry of the microfluidic device was meticulously designed. To make it, a soft lithography method was used. Polymer polydimethylsiloxane (PDMS) was used to fabricate this microfluidic device, sterilized with ethylene oxide gas and following each usage, placed in a clean plastic bag. Because of its favorable mechanical characteristics, elasticity, optical transparency, biocompatibility, and straightforward manufacturing procedure, PDMS was selected for the fabrication of this microfluidic device.

The microfluidic device channel had dimensions of 200 µm width, 150 µm depth, and a total length of 8 mm. The microfluidic device chamber had a diameter of 1300 µm. This microfluidic device comprises two inlets: Inlet A, designed for the input of culture medium flow, and Inlet B, designated for the input of FF-mas. Additionally, it features an outlet for the exit of culture medium flow and FF-mas. The chamber is specifically designed for the collection of mature oocytes.

## **2.7 Evaluating the cellular toxicity of the microfluidic device**

In this study, conducted the Human Sperm Survival Assay (HSSA) to evaluate the device's cytotoxicity. Semen samples were obtained from twelve individuals with normal sperm parameters. These samples were processed in HEPES-buffered medium, and the resulting sperm suspensions were utilized in the HSSA. In the experimental group, the device was aseptically placed in a conical tube containing 1 ml of sperm suspension. In contrast, the control group involved a conical tube with only 1 ml of spermatozoa. The tubes were maintained at room temperature, and sperm suspension samples were gathered at different time intervals: 0, 1, 2, 3, 4, 5, 24, 48, and 72 hours. With a sterile pipette, 10  $\mu$ l of the suspension was dispensed onto a glass slide. Subsequently, a coverslip was positioned over the slide, and scrutinized under a microscope. The Survival Index (SI) was computed by assessing the percentage of progressive motile spermatozoa in the experimental samples. The SI was calculated by dividing the percentage of progressive motile spermatozoa in the experimental group by the corresponding percentage in the control group at the specified time intervals. SI values below 85% indicate potential toxicity. In this study, this cutoff value was utilized to identify potential sperm toxicity<sup>23</sup>.

## 2-8 Experimental design

In this experimental study, GV oocytes were divided into five groups for culture (**Figure 1**). In the first group, GV oocytes were cultured in 25  $\mu$ L drops of culture medium for 24 h at 37°C, 5% O<sub>2</sub>, and 6% CO<sub>2</sub>, with high humidity, under paraffin oil, and without medium renewal. In the second group, GV oocytes were cultured using the same drop culture method as in the first group, with the addition of a 10  $\mu$ M FF-MAS supplement to the culture medium. In the third group, GV oocytes were cultured under dynamic microfluidic conditions for 24 h at 37°C, 5% O<sub>2</sub>, and 6% CO<sub>2</sub>, with high humidity. In this scenario, the GV oocyte was cultured in a device chamber. Inlet A of the microfluidic device, connected to a syringe pump (Mizan Micro Tech model: MMT-SP-102-Iran) via a silicone tube and connector, supplied the culture medium at a flow rate of 6.5  $\mu$ L/min into the device, while Inlet B remained closed. In the fourth group, GV oocytes were also cultured under dynamic microfluidic conditions, following the same design as in the third group. Additionally, at the beginning of the culture, FF-MAS supplement was supplied to the oocytes at a flow rate of 6.5  $\mu$ L/min for a duration of 2 h from input B. The fifth group closely mirrors the fourth group in terms of dynamic microfluidic culture and the presence of the FF-MAS supplement (10  $\mu$ M). However, there is a significant distinction in this group's experimental approach. Instead of a 2 h exposure as in the fourth group, in the fifth group, the FF-MAS supplement is continuously supplied to the oocytes through input B for a prolonged duration of 24 h.

In order to prepare for ICSI insemination, oocyte maturity was evaluated 24 h later by observing the presence of PB1 using an inverted microscope (Nikon Co, Japan)<sup>24</sup>.

## Figure 1.

## 2-9 Fertilization and embryo culture

Fertilization and embryo formation rates were assessed and compared across the different groups. The fertilization rate was determined by calculating the ratio of normally fertilized oocytes to injected

oocytes, while the embryo formation rate was defined as the proportion of cleaved embryos formed to the total number of fertilized oocytes. After ICSI, the embryos were cultured under similar conditions as the oocytes, with the exception that FF-MAS supplement was omitted from the culture medium, and only static and dynamic culture conditions were applied to the embryos. Fertilization status was evaluated 16–18 h after ICSI in each of the five groups, and the fertilized oocytes were subsequently cultured in cleavage medium for 72 h. The development of the embryos was assessed based on grading criteria <sup>25</sup>.

## **2-10 RNA extraction and cDNA synthesis**

RNA extraction was carried out using a RNeasy Micro Kit (Qiagen, Germany) in accordance with the manufacturer's instructions. The purity of samples was evaluated using A260/A280 nm ratio with expected value between 1.8 to 2.0. The purified RNAs were employed for cDNA synthesis using a RevertAid™ H Minus First Strand cDNA Synthesis Kit (Thermo, Lithuania) and random hexamer primers, following the manufacturer's instructions. The reverse transcription was conducted in 20 µL reactions for 60 min at 42 °C, followed by 70 °C for 5 min to deactivate the reverse transcriptase.

## **2-11 Real-Time Polymerase Chain Reaction**

Gene expression was assessed using quantitative Realtime PCR. Primer design of nuclear maturation genes (CDC20-UBA52-TP53-BRCA1), cytoplasmic maturation genes (PAD6-TLE6) and housekeeping gene (GAPDH) was conducted using Primer Design Software (version 6.24; Primer Biosoft, Palo Alto, USA) (**Table 1**). The PCR run was conducted according the Quanti Tect SYBR Green RT-PCR (Applied Biosystems, UK) kit on an Applied Biosystems Step One (Thermo Fisher Scientific, Paisley, UK), following a three-stage protocol: Stage 1: 95 °C for 10 min, stage 2: 95 °C for 15 sec (by 40 cycles) and stage 3: 60 °C for 1 min. The reaction was carried out in triplicates for each sample, with a concurrent run of a no template control alongside the original sample. The Applied Biosystems Step One software (version 2.1; Thermo Fisher Scientific) was utilized to obtain the relative expression of each gene.

### **Table 1.**

## **2-12 Electron microscopy**

A total of 20 oocytes were prepared for transmission electron microscopy (TEM). Among these oocytes, 4 were in immature state (GV), while the remainder were matured using in vitro maturation (IVM) technology within our study groups. Following the methodology outlined by Nottola et al., we processed the oocytes for TEM <sup>26</sup>. Initially, we initiated the fixation process by immersing the oocytes in a solution containing 1.5% glutaraldehyde (Sigma, Mo, USA) in phosphate-buffered saline (PBS). This fixation was conducted for a period ranging from 2 to 5 days at a temperature of 4°C. Subsequently, the oocytes underwent a thorough PBS rinse to eliminate any excess fixative. In the subsequent step, we subjected the samples to post-fixation with 1% osmium tetroxide (Agar Scientific, Stansted, UK) in PBS, followed by another round of rinsing in PBS. The oocytes were subsequently gently embedded in small blocks composed of 1% agar (Sigma, Mo, USA). These embedded samples were progressively dehydrated

through exposure to an ascending ethanol series and immersed in propylene oxide for solvent substitution. The final step involved embedding the samples in Araldite resin (Merk, Germany). Afterwards, the samples were sectioned, producing slices ranging from 0.5 to 1  $\mu\text{m}$  in thickness, which were subsequently stained with Toluidine blue. These stained sections were examined under a light microscope (Zeiss Axioskop). ultrathin sections, were cut between 60-80 nm, mounted on copper grids, and subjected to contrast enhancement using uranyl acetate and lead citrate. Finally, these ultrathin sections were scrutinized and photographed utilizing a TEM operating at 80 kV (Zeiss, Germany).

**2-13 Statistical Analysis**

The data are presented as mean  $\pm$  SD. Fisher’s exact test and One sample t test were used appropriately. To assess the distribution of the data, the D'Agostino-Pearson test was employed. All hypotheses were two sided and the significant level was defined as  $p < 0.05$ . Also, Statistical analysis was carried out using GraphPad Prism version 8.4.2 (GraphPad Software, Inc., San Diego, CA).

**Results**

**3.1 Microfluidic device toxicity test**

The ratio of sperms with progressive motile in the experimental group to the control group was computed at the specified time spans in order to obtain Survival Index (SI) (**Table 2**). The survival index was not less than 85% in any of the evaluated time points.

**Table 2.**

**3.2 Evaluation of maturation, fertilization, and embryo development**

A total of 438 immature oocytes were collected based on predefined exclusion criteria. Following denudation of COC and morphological evaluation<sup>27</sup>, 32 GV oocytes were excluded. Subsequently, 406 GV oocytes with normal morphology were included in the study. The assessment of maturity for immature oocytes was conducted 24 h later. The maturation rates for rescue IVM oocytes in the first (control), second, third, fourth, and fifth groups were 36%, 48%, 42%, 64%, and 65%, respectively (**Fig. 2A**). The results demonstrated a significant increase in maturation rates in the fourth and fifth groups compared to the control, second, and third groups ( $p < 0.05$ ). Furthermore, normal fertilization rates in the fourth and fifth groups exhibited a significant difference compared to the control and second groups ( $p < 0.05$ ) (**Fig. 2B**). No statistically significant differences were observed between the groups with respect to embryo formation rates (**Fig. 2C**). However, the formation of high-quality embryos in groups three, four, and five exhibited a significant increase compared to the control and second groups ( $p < 0.05$ ) (**Fig. 2D**). These findings are summarized in **Table 3**.

**Figure 2.**

**Table 3.**



### 3.3 Gene expression evaluation of maturation oocytes

The study investigated the mRNA levels of key nuclear and cytoplasmic maturation-related genes in experimental groups using comparative real-time PCR. Specifically, genes such as CDC20, UPA52, TP53, BRCA1 (**Fig. 3A, B, C, D**), PADI6, and TLE6 (**Fig. 3E, F**) were analyzed. The expression levels of genes associated with the spindle checkpoint (CDC20) and cell cycle regulation (UBA52) did not show significant differences when comparing the experimental groups to the control groups. However, distinct expression patterns were observed in the DNA repair gene (BRCA1) in the third, fourth, and fifth groups compared to the control group ( $p < 0.05$ ). Similarly, the expression of the DNA damage response and cell cycle regulation gene (TP53) demonstrated a significant difference in the third, fourth, and fifth groups compared to the control group ( $p < 0.05$ ). Furthermore, in the genes related to cytoplasmic maturation (PADI6, TLE6), a noteworthy increase in expression levels was evident in the third, fourth, and fifth groups as compared to the control group ( $p < 0.05$ ).

#### Figure 3.

### 3.4 Ultrastructural features

Investigating ultrastructure images of mature oocytes across distinct experimental groups, we observed a uniform dispersion of detectable organelles throughout the entire cell volume, a consistent feature across all groups (**Fig 4A**). Upon closer examination, the zona pellucida was identified as composed of electron-dense fibrous materials, forming a complete enclosure around the oocyte and separated by a narrow perivitelline space (PVS) from the oolemma. The oolemma in all oocytes exhibited extension and numerous microvilli that reached into the PVS. Additionally, cortical granules (CG), characterized by their round and electron-dense nature, were observed in a layer beneath the oolemma (**Fig 4B**).

#### Figure 4.

The observable cytoplasmic organelles in our samples were predominantly mitochondria and endoplasmic reticulum (ER). Mitochondria were found to be the most prevalent organelles in oocytes at all stages of maturation. Unlike the rod-shaped organelles with a typically wrinkled inner membrane, the oocytes displayed round-to-oval mitochondria with a dense matrix and sparse, either parallel or transversal, cristae (**Fig. 5A**). The morphology and quantity of the mitochondria did not appear to undergo significant changes during meiotic maturation. In MII oocytes, the cortical region was populated by numerous mitochondria, which exhibited a tendency to approach randomly distributed ER structures. A common feature in oocytes matured under dynamic conditions groups is the presence of a higher proportion of aggregates of anastomosing tubules of smooth endoplasmic reticulum (SER) surrounded by mitochondria (M-SER aggregates), forming "necklace-like" complexes composed of a spherical sac SER adorned with circular mitochondria (**Fig. 5B, C**). In contrast, in oocytes matured under static conditions, a higher proportion of small vesicles containing a slightly electron-dense material were associated with mitochondria, forming more mitochondria-vesicles (MV) complexes (**Fig. 5D**). Notably,

individual ribosomes, polyribosomal complexes, or rough ER were not readily detectable in our TEM images.

Unlike mature oocytes, GV oocytes exhibited a non-homogeneous distribution of organelles throughout the cytoplasm, with a notable concentration in the perinuclear region. The individual mitochondria and small mitochondrial clusters were concentrated in the perinuclear area (**Fig. 5E**). Unlike in somatic cells, the cistrans polarity of Golgi apparatus was not easily distinguishable in oocytes. The Golgi apparatus remnants were never in MII oocytes. This observation supports the notion that Golgi apparatus undergoes progressive disintegration in the course of maturation (**Fig. 5F**).

**Figure 5.**

## Discussion

The rescue of immature oocytes is crucial, especially when dealing with a large number of oocytes obtained from PCOS patients. Elevating oocyte competence and perfecting the in vitro maturation process requires a transformation of static oocyte culturing systems to faithfully emulate the dynamic environment of the mammalian female reproductive tract. This transformation aims to replicate the natural conditions of the ovary and fallopian tube, providing the necessary factors and supplements to increase the resumption of oocyte meiosis and enhance the quality of mature oocytes. In this study, we aimed to replicate the natural conditions of the ovary and fallopian tube, optimizing the in vitro maturation process and enhancing oocyte competence. Our innovative approach involved the design and construction of an in vitro model that replicates natural conditions to investigate the effect of the FF-MAS supplement on the maturation rate of immature oocytes in individuals with PCOS under in vitro conditions using a microfluidic device.

In our study, we observed a significant correlation between the duration of oocyte culture in laboratory conditions and the quality of mature oocytes, as well as the subsequent development of embryos. Our findings suggest that the highest rate of rescued oocyte maturation occurs within 24 hours of culture.

To mitigate the potential impact of incubation timing on chromosomal abnormalities, we established a critical maturation time of 24 hours for rescuing IVM oocytes<sup>28</sup>. In line with our findings, Zhang et al. reported that embryos derived from oocytes that matured 48 hours after collection exhibited higher rates of chromosomal abnormalities compared to embryos derived from in-vivo matured oocytes and those derived from oocytes that matured within the first 24 hours after collection. Their study supports the preferential transfer of embryos derived from 24-hour matured oocytes in IVM cycles<sup>28</sup>.

The proper maturation of the oocyte to metaphase II is essential for fertilization and preimplantation development. Our study's findings revealed a significant increase in the rate of oocyte maturation and fertilization in the fourth and fifth experiment groups compared to the other groups. Concordant with our findings, Hester and coworkers conducted a study aligning with our research focus. They reported a significant enhancement in the maturation rate of porcine oocytes cultured in PDMS glass

microchannels when compared to those matured in 500 µl droplets <sup>29</sup>. Similarly, Oskouei and colleagues, in their article, assessed mouse oocyte maturation in dynamic culture systems versus conventional static culture. Their results demonstrated significantly higher percentages of mature oocytes and lower rates of oocyte arrest and degeneration in the dynamic culture systems. Moreover, the fertilization and blastocyst formation rates in the dynamic systems exhibited statistical significance when compared to the static cultures <sup>30</sup>. The observed improvement can be attributed to the implementation of a dynamic microfluidic environment specifically designed to replicate the natural conditions present within the ovary and fallopian tube. The unique environment provided by the fourth and fifth experimental groups facilitated a more physiologically relevant setting for oocyte maturation, resulting in enhanced maturation efficiency and subsequent embryo development. This underscores the potential of the microfluidic environment in improving oocyte maturation rates and overall fertilization outcomes. Furthermore, the dynamic microfluidic environment ensured a continuous and controlled supply of FF-MAS to the oocytes, mimicking the in vivo conditions experienced during the initial hours of transit through the fallopian tube. This continuous exposure to FF-MAS may effectively support the resumption of oocyte meiosis and contribute to enhancing the quality of mature oocytes compared to static culture conditions.

The formation of embryos from the matured oocytes in the experimental groups was investigated until the third day. The results showed that while the rates of embryo formation were similar across all groups, the rates of high-quality embryo formation in the third, fourth, and fifth groups exhibited a significant increase compared to the control and second groups. Our study's findings are consistent with those of Raty and colleagues, who demonstrated that mouse embryos cultured in microchannels displayed faster cleavage rates, reduced embryo degeneration, and increased high-quality embryo formation compared to embryos cultured in control microdrops <sup>31</sup>. The noticeable increase in the rates of high-quality embryo formation in the dynamic experimental groups compared to the static groups can be attributed to key factor identified in our study. Certain metabolites, essential during one developmental phase, may become redundant in others. Consequently, their accumulation could potentially diminish embryo quality. Also, the static groups experience increased accumulation of ROS, leading to higher embryo fragmentation and a subsequent reduction in embryo quality. In the dynamic groups, however, the concentration of ROS generated through dynamic flow diminishes, resulting in a lower rate of embryo fragmentation and an increase in the production of high-quality embryos <sup>32</sup>.

It appears that the accumulated ROS in groups subjected to static conditions also influences the molecular mechanisms associated with embryo quality.

Molecular study of the related genes revealed a significant decrease in the BRCA1 gene in the dynamic culture groups. Since the BRCA1 gene is associated with cell DNA repair <sup>33</sup>, our findings suggest that in the static culture groups, the increased accumulation of ROS and its destructive role in embryo cell DNA lead to an upregulation in the expression of the BRCA1 gene compared to the dynamic culture group. Furthermore, TP53 plays a pivotal role in cellular responses to DNA damage. BRCA1 regulates

TP53 under stress, implying that TP53 initiates the DNA repair pathway instead of the apoptotic pathway<sup>34</sup>. In our study, the higher expression of BRCA1 relative to TP53 in the second group suggests that TP53 has activated the DNA repair pathway rather than the apoptotic pathway. Additionally, the comparison of BRCA1 to TP53 expression in the third, fourth, and fifth groups indicates that, due to reduced DNA damage in these groups, the levels of BRCA1 and TP53 show no significant differences. Consistent with our findings, Wells et al. demonstrated an evident inverse relationship in the expression of BRCA1 and TP53 genes, indicating the presence of an intracellular TP53/BRCA1 pathway in response to various stress conditions<sup>35</sup>.

In our examination of other genes associated with nuclear maturation, our analysis revealed that both the CDC20 gene, implicated in the spindle checkpoint, and the UBA52 gene, associated with cell cycle regulation, did not exhibit statistically significant differences between the experimental and control groups. However, it is plausible to anticipate an upregulation of these genes in mature MII oocytes within the experimental groups, in contrast to the immature GV oocytes. Drawing upon the findings of Hoseini and colleagues, who observed elevated expression of CDC20 in mature oocytes compared to immature GV oocytes, our study aligns with the notion that CDC20 plays a crucial role in the resumption of meiosis by affecting the spindle checkpoint<sup>36</sup>. Additionally, Virant-Klun and colleagues, found increased expression of the UBA52 gene in mature oocytes compared to immature oocytes, further emphasizing its essential role in regulating the cell cycle and facilitating the resumption of meiosis<sup>37</sup>.

In the investigation of genes associated with cytoplasmic maturation, our analysis revealed a noteworthy increase in the expression of PADI 6 and TLE6 genes within the third, fourth, and fifth groups, as compared to the control group. Considering the substantial rearrangement of organelles during oocyte cytoplasmic maturation within a voluminous context<sup>38</sup> it is reasonable to hypothesize that mature oocytes in dynamic culture conditions with increased expression of this genes may have created special structures to facilitate the position and distribution of organelles that help the formation of competent oocytes. Recent studies propose that oocyte cytoplasmic lattices (CPLs), particularly with the involvement of the PADI6 gene, play a crucial role in facilitating the distribution of organelles<sup>39</sup>. Consequently, these findings, alongside others, suggest the intriguing possibility that these lattices may directly influence microtubule (MT)-mediated organelle distribution during oocyte cytoplasmic maturation<sup>39</sup>.

Studies demonstrate that TLE6, as a maternal factor, is crucial for both oocyte cytoplasmic maturation and developmental progression beyond the 2-cell stage<sup>40</sup>. Intriguingly, PADI6 and TLE6 have been identified as members of a high molecular weight complex known as the subcortical maternal complex (SCMC)<sup>41</sup>. A wealth of evidence now links the expression of various SCMC components to oocyte developmental competence. The SCMC appears to play a role in translocating organelles to the subcortical region of the oocyte at specific times, possibly through its functional interaction with the F-actin meshwork via Cofilin<sup>41</sup>. This suggests that the dynamic microfluidic culture medium might be influencing the intricate dynamics of the SCMC, subsequently impacting the translocation of organelles

within the oocyte cytoplasm. Building upon these findings, noteworthy research conducted by Fernandez and colleagues has illuminated a compelling relationship between the SCMC and the precise distribution of mitochondria in mature oocytes. Their work underscores the fundamental significance of proper mitochondrial localization in mature oocytes, emphasizing its crucial role in signaling events associated with fertilization and developmental competence <sup>42</sup>.

In examinations of ultrastructure, the normalcy of cortical granules and the absence of ultrastructural changes between the control and experimental groups underscore the stability and resilience of oocyte ultrastructure in different experimental conditions. It is evident that during the GV stage, CG are few in number and located in the innermost part of the cytoplasm before being moved closer to the oolemma during maturation <sup>43</sup>. Thus, in the maturation conditions adopted in our study, the overall process of CG migration seemed to occur normally for the vast majority. Wessel and colleagues reported that cortical granules are Golgi-derived, membrane-bound spherical or slightly ellipsoidal organelles. The exocytosis of cortical granule contents into the PVS immediately after oocyte fertilization leads to changes in the ZP glycoproteins, establishing the block to polyspermy <sup>44</sup>. Additionally, the intact oolemma and well-distributed microvilli observed in all groups align with established prerequisites for successful spermatozoon-oocyte fusion, suggesting a robust foundation for fertilization processes. The morphology of mitochondria in the control group and other experimental groups appeared to be unaffected by the culture conditions. They exhibited consistent shapes, sizes, internal architectures, and textures. A study by Yang and colleagues reported the presence of swollen mitochondria with indistinct cristae and signs of apoptosis in oocytes matured in vitro <sup>45</sup>. However, interpreting such findings is challenging as the immature oocytes were leftovers from a single stimulated cycle, and no in vivo matured oocytes were evaluated for comparison.

Oocytes matured in dynamic condition displayed numerous M-SER aggregates, acting as reservoirs of energy, nutrients, and factors crucial for fertilization <sup>46</sup>. However, oocytes matured in static condition showed a reduced presence of M-SER aggregates, seemingly replaced by MV complexes. In the study conducted by Coticchio and colleagues, their results underscore the potential influence of static oocyte culture conditions on the development of M-SER aggregates. The study indicates a decrease in the presence of these structures, seemingly supplanted by MV complexes <sup>43</sup>. Thus, it is hypothesized that oocytes cultured under static conditions may not reach complete cytoplasmic maturation, and the delay in this maturation process may contribute to the prevalence of these complexes in mature oocytes. The altered ratios of M-SER aggregates /MV complexes observed in mature oocytes under different culture conditions could negatively affect the oocyte's ability to be fertilized. As a precautionary note, it is important to highlight that the analysis was conducted on a small number of MII oocytes under different culture conditions. Further investigation is needed to confirm whether these findings accurately represent the broader population.

## Conclusion

In this study, we have developed a novel microfluidic device designed for immature oocyte culture with the aim of emulating the natural ovary and fallopian tube environment to enhance fertility treatment outcomes. The device's straightforward architecture, chip design, and programmable fluid actuation enable precise manipulation of chemical and mechanical microenvironments for in vitro oocyte maturation. Our findings indicate that the dynamic culture and the inclusion of the FF-MAS factor in the in vitro oocyte maturation process lead to a significant increase in MII obtained oocytes compared to the traditional static culture system. Furthermore, this approach demonstrates enhanced fertilization rates and a heightened formation of high-quality embryos. This research underscores the potential of the newly fabricated microfluidic device to positively impact fertility treatment outcomes by providing a conducive environment for oocyte maturation and improving the overall success rate of the treatment process.

## Declarations

### Data availability

All the data are available from the corresponding author upon request.

### Author contributions statement

H.T., R.Sh., T.A. and M.M. designed this project. H.T. and R.Sh. drafted the manuscript. T.A. and Sh.P. contributed extensively to the interoperation of the data collection and statistical analysis. M.Mo. made significant contributions to the development of the microfluidic device. M.M. and R.Sh. interpretation of the data and presented a critical revision of the draft. All authors read and approved the final manuscript.

### Competing interests

The authors declare no competing interests.

## References

1. Alikhani, M. *et al.* Proteome analysis of endometrial tissue from patients with PCOS reveals proteins predicted to impact the disease. *Mol. Biol. Rep.* **47**(11), 8763–8774 (2020).
2. Rudnicka, E., Duszewska, A. M., Kucharski, M., Tyczyński, P. & Smolarczyk, R. Oxidative Stress and Reproductive Function: Oxidative stress in polycystic ovary syndrome. *Reproduction* **164**(6), F145–F154 (2022).
3. Singh, S. *et al.* Polycystic ovary syndrome: etiology, current management, and future therapeutics. *J. Clin. Med.* **12**(4), 1454 (2023).
4. Chian, R., Li, J., Lim, J. & Yoshida, H. IVM of human immature oocytes for infertility treatment and fertility preservation. *Reprod. Med. Biol.* **22**(1), e12524 (2023).

5. Rodrigues, P. *et al.* In vitro maturation of oocytes as a laboratory approach to polycystic ovarian syndrome (PCOS): From oocyte to embryo. *WIREs Mech. Dis.* **15**(3), e1600 (2023).
6. Rose, B. I. & Nguyen, K. The effect of in vitro maturation (IVM) protocol changes on measures of oocyte/embryo competence. *Reprod. Med.* **4**(1), 65–73 (2023).
7. Grøndahl, C. Oocyte maturation. Basic and clinical aspects of in vitro maturation (IVM) with special emphasis of the role of FF-MAS. *Dan. Med. Bull.* **55**(1), 1–16 (2008).
8. Guo, R. *et al.* Follicular fluid meiosis-activating sterol (FF-MAS) promotes meiotic resumption via the MAPK pathway in porcine oocytes. *Theriogenology* **148**, 186–193 (2020).
9. Bokal, E. V. *et al.* Follicular sterol composition in gonadotrophin stimulated women with polycystic ovarian syndrome. *Mol. Cell. Endocrinol.* **249**(1-2), 92–98 (2006).
10. Dang, K. N. *et al.* Follicular Fluid Meiosis-Activating Sterol in Assisted Reproductive Techniques: A Systematic Review and Meta-analysis of Randomized Controlled Trials. *Fertil. Reprod.* **2**, 144–159 (2020).
11. Yuan, Y., Paczkowski, M., Wheeler, M. B. & Krisher, R. L. Use of a novel polydimethylsiloxane well insert to successfully mature, culture and identify single porcine oocytes and embryos. *Reprod. Fertil. Dev.* **26**(3), 375–384 (2014).
12. Oskouei, B. S., Zargari, S., Shahabi, P., Novin, M. G. & Pashaiasl, M. Design and microfabrication of an on-chip oocyte maturation system for reduction of apoptosis. *Cell J.* **23**(1), 32-39 (2021).
13. Liu, Q., Zhao, S., Zhou, J., Liu, P. & Huo, B. Effects of microvibration stimulation on developmental potential of discarded germinal vesicle oocytes of human. *Front. Endocrinol. (Lausanne)*. **13**, 1028557 (2022).
14. Bahrami, M. & Cottee, P. A. Culture conditions for in vitro maturation of oocytes—A review. *Reprod. Breed.* **2**, 31–36 (2022).
15. Smith, G. D. & Takayama, S. Application of microfluidic technologies to human assisted reproduction. *MHR Basic Sci. Reprod. Med.* **23**(4), 257–268 (2017).
16. Yanez, L. Z. & Camarillo, D. B. Microfluidic analysis of oocyte and embryo biomechanical properties to improve outcomes in assisted reproductive technologies. *MHR Basic Sci. Reprod. Med.* **23**(4), 235–247 (2017).
17. Ferraz, M. de A. M. M. & Ferronato, G. de A. Opportunities involving microfluidics and 3D culture systems to the in vitro embryo production. *Anim. Reprod.* **20**(2), e20230058 (2023).
18. Sequeira, R. C., Criswell, T., Atala, A. & Yoo, J. J. Microfluidic systems for assisted reproductive technologies: Advantages and potential applications. *Tissue Eng. Regen. Med.* **17**(6), 787–800 (2020).
19. ESHRE, T. R. & Group, A.-S. P. C. W. Revised 2003 consensus on diagnostic criteria and long-term health risks related to polycystic ovary syndrome. *Fertil. Steril.* **81**(1), 19–25 (2004).
20. Tabatabaie, M. *et al.* The effect of Myo-Inositol supplement on molecular regulation of folliculogenesis, steroidogenesis, and assisted reproductive technique outcomes in patients with

- polycystic ovarian syndrome. *Mol. Biol. Rep.* **49**(2), 875–884 (2022).
21. Baltsen, M. & Byskov, A. G. Quantitation of meiosis activating sterols in human follicular fluid using HPLC and photodiode array detection. *Biomed. Chromatogr.* **13**(6), 382–388 (1999).
  22. Croxatto, H. B. Physiology of gamete and embryo transport through the Fallopian tube. *Reprod. Biomed. Online* **4**(2), 160–169 (2002).
  23. Lierman, S., De Sutter, P., Dhont, M. & Van der Elst, J. Double-quality control reveals high-level toxicity in gloves used for operator protection in assisted reproductive technology. *Fertil. Steril.* **88**(4), 1266–1272 (2007).
  24. Dale, B. & Elder, K. Oocyte retrieval and embryo culture. in *In-Vitro Fertilization* (eds. Dale, B. & Elder, K.) 157–190 (Cambridge University Press, 2010).
  25. Bączkowski, T., Kurzawa, R. & Głabowski, W. Methods of embryo scoring in in vitro fertilization. *Reprod. Biol.* **4**(1), 5–22 (2004).
  26. Nottola, S. A. *et al.* Ultrastructural markers of quality in human mature oocytes vitrified using cryoleaf and cryoloop. *Reprod. Biomed. Online* **19**, 17–27 (2009).
  27. Rienzi, L., Balaban, B., Ebner, T. & Mandelbaum, J. The oocyte. *Hum. Reprod.* **27**, i2–i21 (2012).
  28. Zhang, X. Y. *et al.* Chromosome abnormality rates in human embryos obtained from in-vitro maturation and IVF treatment cycles. *Reprod. Biomed. Online* **21**(4), 552–559 (2010).
  29. Hester, P. N. *et al.* Enhanced cleavage rates following in vitro maturation of pig oocytes within polydimethylsiloxane-borosilicate microchannels. *Theriogenology* **57**, 723 (2002).
  30. Oskouei, B. S. *et al.* Evaluation of mouse oocyte in vitro maturation developmental competency in dynamic culture systems by design and construction of a lab on a chip device and its comparison with conventional culture system. *Cell J.* **18**(2), 205–213 (2016).
  31. Raty, S. *et al.* Embryonic development in the mouse is enhanced via microchannel culture. *Lab Chip* **4**(3), 186–190 (2004).
  32. Wang, M. *et al.* Oviduct-mimicking microfluidic chips decreased the ROS concentration in the in vitro fertilized embryos of CD-1 mice. *Biomed. Pharmacother.* **154**, 113567 (2022).
  33. Martin, J. H., Aitken, R. J., Bromfield, E. G. & Nixon, B. DNA damage and repair in the female germline: contributions to ART. *Hum. Reprod. Update* **25**(2), 180–201 (2019).
  34. Assou, S. *et al.* The human cumulus–oocyte complex gene-expression profile. *Hum. Reprod.* **21**(7), 1705–1719 (2006).
  35. Wells, D. *et al.* Expression of genes regulating chromosome segregation, the cell cycle and apoptosis during human preimplantation development. *Hum. Reprod.* **20**(5), 1339–1348 (2005).
  36. Hoseini, F. S., Salsabili, N., Akbari-Asbagh, F., Aflatoonian, R. & Aghaee-Bakhtiari, S. H. Comparison of gene expression profiles in human germinal vesicle before and after cytoplasmic transfer from mature oocytes in Iranian infertile couples. *J. Fam. Reprod. Heal.* **10**(2), 71–79 (2016).
  37. Virant-Klun, I., Knez, K., Tomazevic, T. & Skutella, T. Gene expression profiling of human oocytes developed and matured in vivo or in vitro. *Biomed Res. Int.* **2013**, 879489 (2013).



38. Ferrer-Vaquer, A., Barragán, M., Rodríguez, A. & Vassena, R. Altered cytoplasmic maturation in rescued in vitro matured oocytes. *Hum. Reprod.* **34**(6), 1095–1105 (2019).
39. Kan, R. *et al.* Regulation of mouse oocyte microtubule and organelle dynamics by PADI6 and the cytoplasmic lattices. *Dev. Biol.* **350**(2), 311–322 (2011).
40. Fei, C. & Zhou, L. Gene mutations impede oocyte maturation, fertilization, and early embryonic development. *Bioessays* **44**(10), e2200007 (2022).
41. Bebbere, D., Masala, L., Albertini, D. F. & Ledda, S. The subcortical maternal complex: multiple functions for one biological structure? *J. Assist. Reprod. Genet.* **33**(11), 1431–1438 (2016).
42. Fernandes, R. *et al.* NLRP5 mediates mitochondrial function in mouse oocytes and embryos. *Biol. Reprod.* **86**(5), 131–138 (2012).
43. Coticchio, G. *et al.* Ultrastructure of human oocytes after in vitro maturation. *MHR Basic Sci. Reprod. Med.* **22**(2), 110–118 (2016).
44. Wessel, G. M. *et al.* The biology of cortical granules. *Int. Rev. Cytol.* **209**, 117–206 (2001).
45. Yang, Y., Zhang, Y. & Li, Y. Ultrastructure of human oocytes of different maturity stages and the alteration during in vitro maturation. *Fertil. Steril.* **92**(1), 396.e1-6 (2009).
46. Familiari, G., Heyn, R., Relucenti, M., Nottola, S. A. & Sathananthan, A. H. Ultrastructural Dynamics of Human Reproduction, from Ovulation to Fertilization and Early Embryo Development. *Int. Rev. Cytol.* **249**, 53–141 (2006).

## Tables

**Table1.** Gene accession number, primer sequence and product size

Gene name	Accession no.	Primer	Amplicon Size (bp)
CDC20	NM_001255	R: GACCACTCCTAGCAAACCTGG F: GGGCGTCTGGCTGTTTTCA	118
TP53	NM_0014477	R: AACTGCGGGACGAGACAGA F: AGCTTCAAGAGCGACAAGTTTT	91
BRCA1	NM_004656	R: GATACGTCCGTGATTGATGATGA F: TGAGTTGCACAAGAGTTGGGTA	80
UBA52	NM_001033930	R: AAGACAAGGAGGGTATCCAC F: TGTTGTAGTCTGAGAGAGTGCG	90
PADI6	NM_207421	R: ATGCCGTTTGTGTGTTGGG F: TCTCAGAAATCACCGTGTGG	132
TLE6	NM_001143986	R: AGCCTCTCGGTTTCTACAGTC F: GGACGGCGAGTCTCTTTGA	104
GAPDH	NM_001289746	R: TGGTATCGTGGAAGGACTCA F: CCAGTAGAGGCAGGGATGAT	132

**Table 2.** Human sperm survival assay was conducted to assess the toxicity of microfluidic device.

Time Items	0 hr	1 hr	2 hr	3 hr	4 hr	5 hr	24 hr	48 hr	72 hr
Control	74%	71%	67%	63%	60%	58%	54%	44%	38%
Test	74%	69%	65%	64%	57%	54%	50%	47%	42%
Survival index	1.00	0.97	0.97	1.01	0.95	0.93	0.92	1.06	1.10
Pass	✓	✓	✓	✓	✓	✓	✓	✓	✓
Fail									

**Table 3.** Conducting a descriptive analysis of maturation, fertilization, embryo development and high-quality embryo rates derived from mature oocytes within controlled laboratory settings across five experimental groups.

	Group 1 (Control)	Group 2	Group 3	Group 4	Group 5
Maturation rate, (matured oocytes/total GV oocytes)	36%, (28/78)	48%, (40/85)	42%, (33/80)	64%, (53/83)	65%, (52/80)
Fertilization rate, (Normal fertilized oocytes/injected oocytes)	48%, (13/27)	45%, (18/40)	63%, (21/33)	72%, (37/51)	70%, (35/50)
Embryo formation rate, (cleaved embryos/total fertilized oocytes)	84%, (11/13)	88%, (16/18)	95%, (20/21)	94%, (35/37)	91%, (32/35)
High-quality embryos formation rate, (grade A+ B embryo/ total fertilized oocyte)	45%, (5/11)	56%, (9/16)	90%, (18/20)	91%, (32/35)	93%, (30/32)

Figures

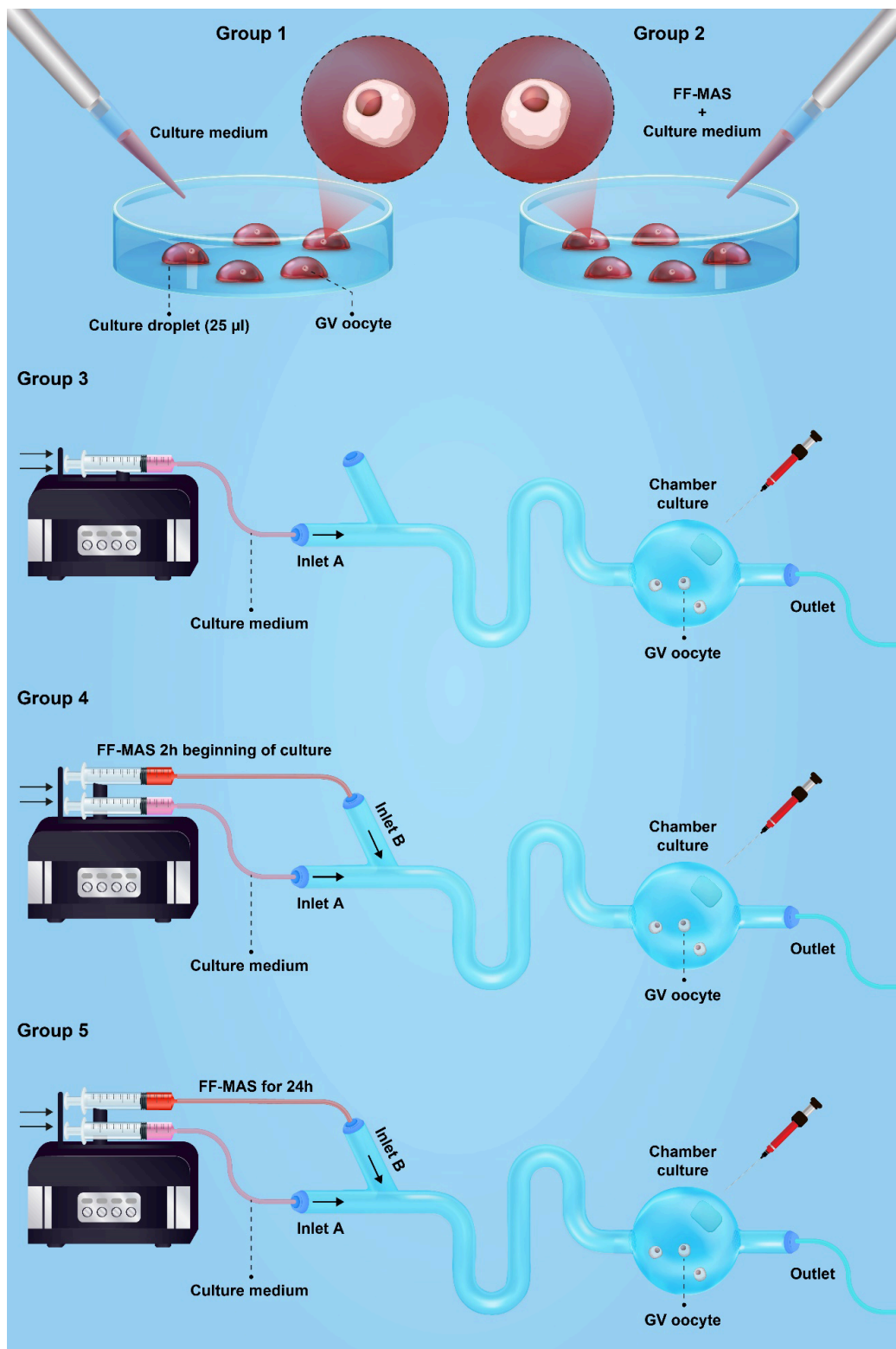


**Figure 1**

Experimental Design Overview. GV oocytes were distributed across five distinct culture conditions. Group 1: Oocytes cultured in 25  $\mu$ L drops of medium for 24 h under static conditions. Group 2: Similar culture as Group 1, with the addition of a 10  $\mu$ M FF-MAS supplement. Group 3: Oocytes cultured in a dynamic microfluidic environment for 24 h. Group 4: oocytes were cultured dynamically for 24 h. During the first 2 h, FF-MAS supplement was introduced through Inlet B. Group 5: Similar to Group 4, oocytes underwent

dynamic microfluidic culture for 24 h. However, in Group 5, FF-MAS supplement was continuously supplied to the oocytes through Inlet B for the entire 24 h duration. This design allows the exploration of the impact of varying culture conditions on oocyte development and maturation.

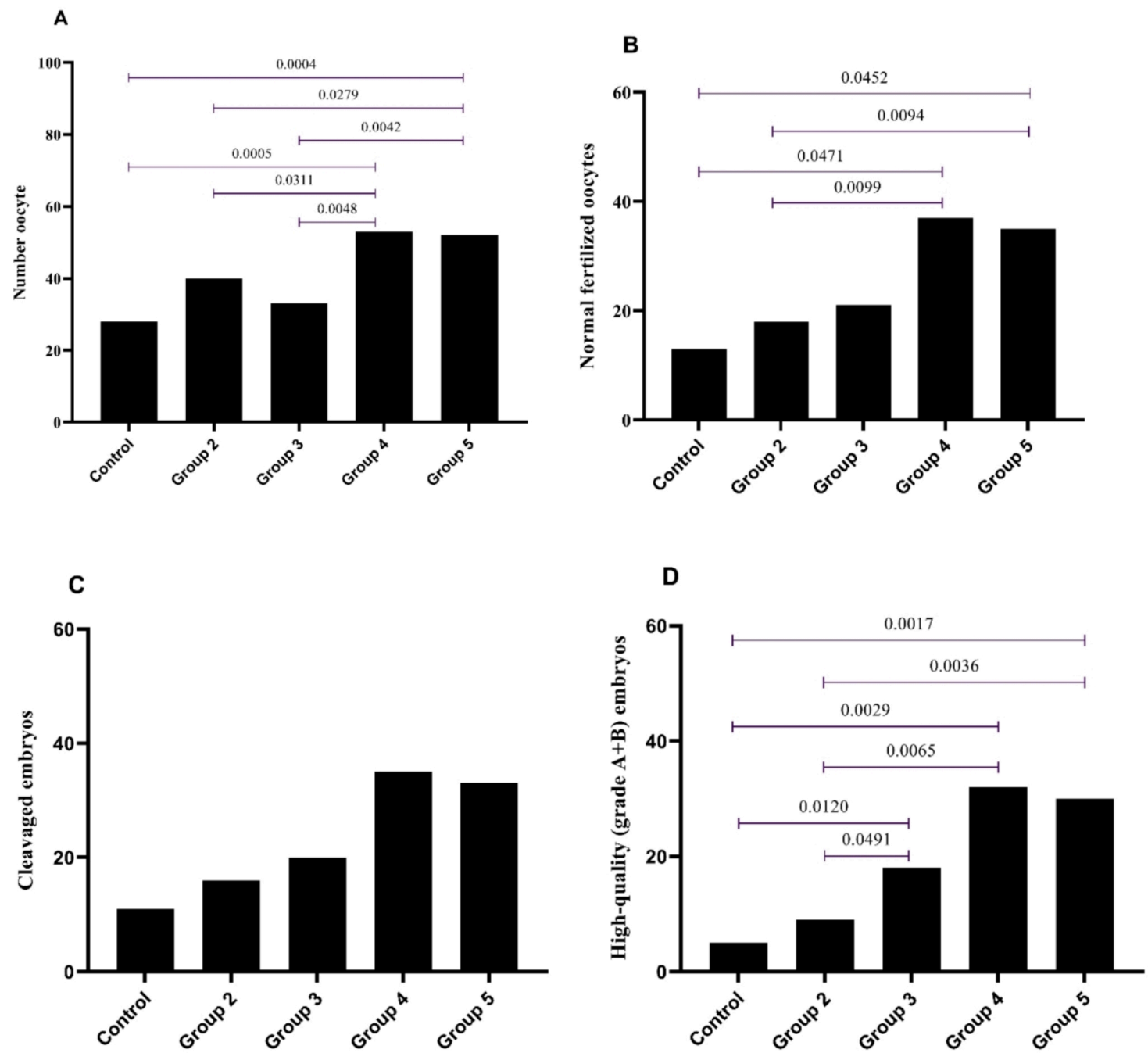
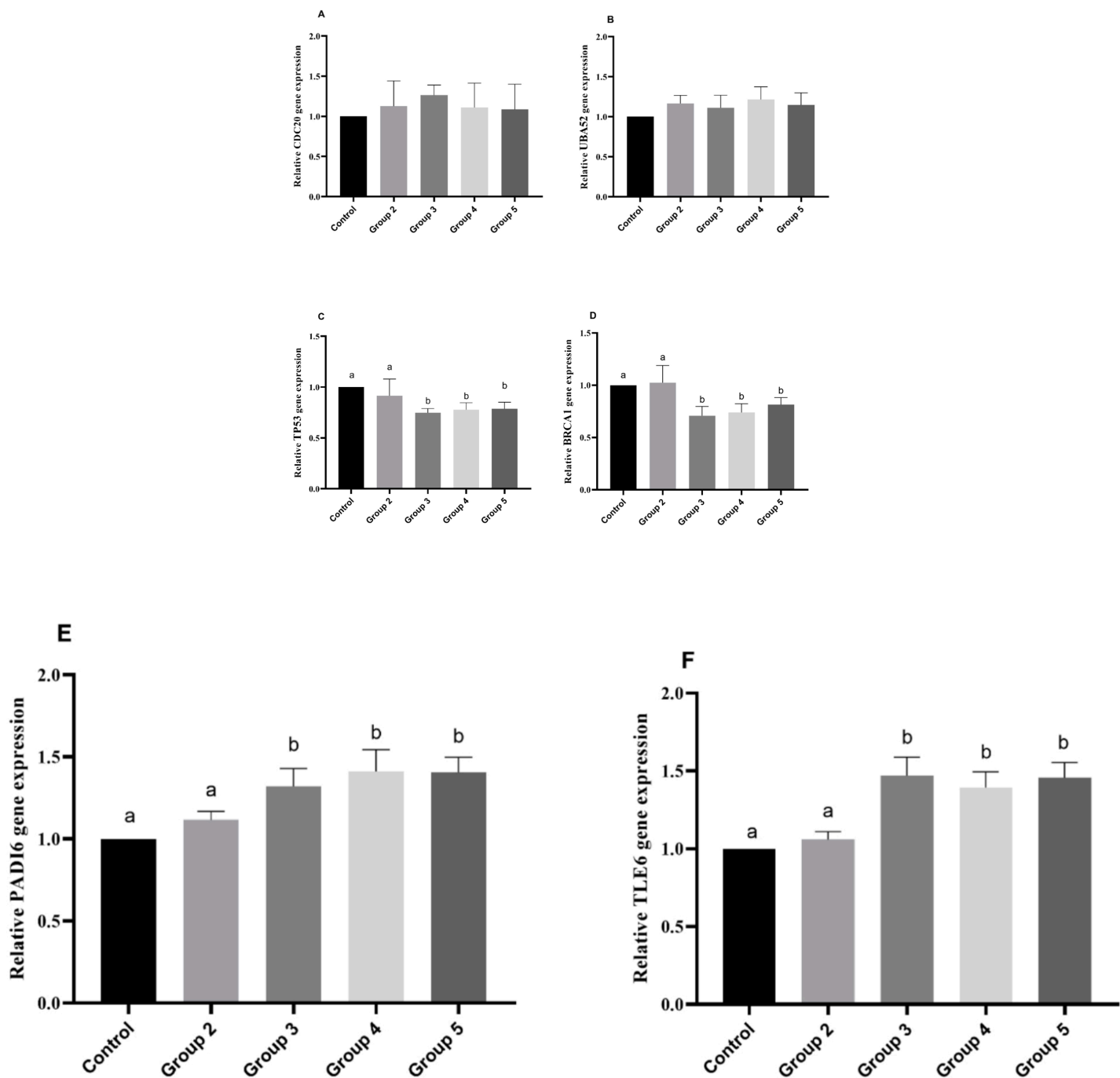


Figure 2

Evaluation of oocyte maturation, fertilization, embryo formation, and high-quality embryo rates across five groups. A) Maturation rates significantly increased in the fourth and fifth groups compared to the control, second, and third groups. B) Fertilization rates in the fourth and fifth groups showed a significant increase compared to those in the control and second groups. C) No significant differences were observed in embryo formation rates among the groups. D) The formation of high-quality embryos in

groups three, four, and five was significantly higher than that in the control and second groups. Statistical analysis employed Fisher’s exact test, and significance was set at ( $p < 0.05$ ).



**Figure 3**

Gene expression levels in experimental groups were compared using real-time PCR. **A** CDC20; **B** UPA52; **C** TP53; **D** BRCA1; **E** PADI6; **F** TLE6 in human oocyte mature in group1,2,3,4 and 5. Statistical analysis utilized a one-sample t-test. Groups followed by same letter were not significantly different at the 0.05 level.

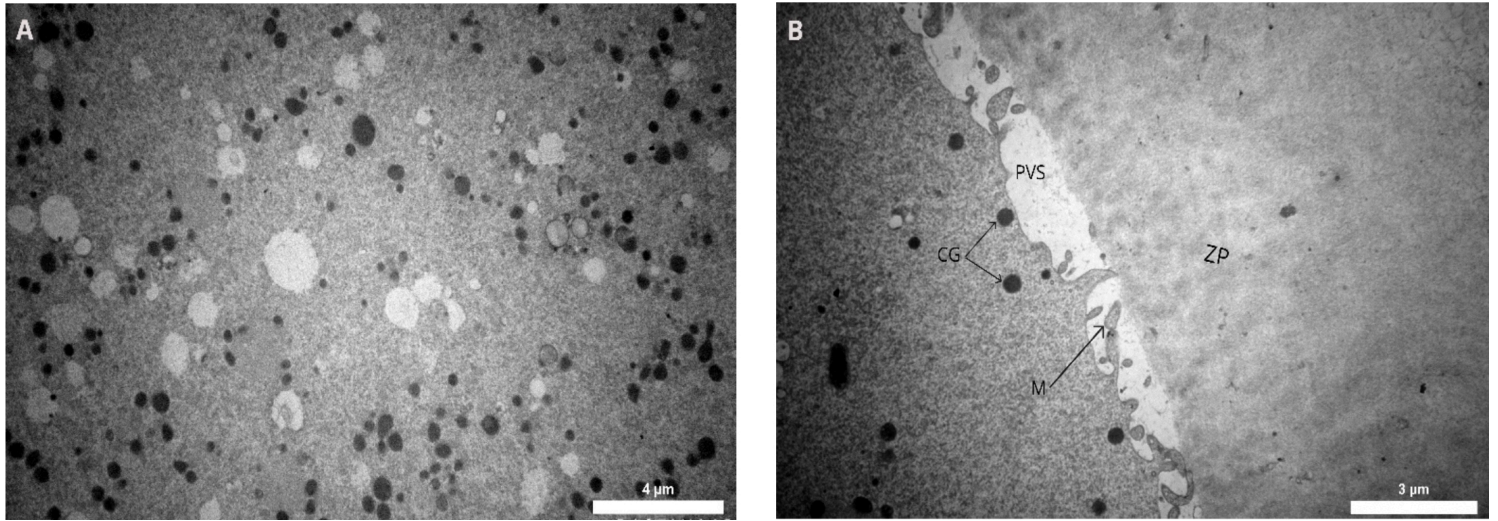


**Figure 4**

Transmission Electron Microscopy (TEM) images illustrating the ultrastructure of mature oocytes. A) Uniform dispersion of detectable organelles throughout the cell volume. B) Zona pellucida composed of electron-dense fibrous materials, forming a complete enclosure around the oocyte with a narrow perivitelline space separating it from the oolemma. Oolemma extension with numerous microvilli reaching into the perivitelline space. Cortical granules, characterized by their round and electron-dense nature, arranged in a layer beneath the oolemma. ZP = zona pellucida; m = microvilli; CG = cortical granules; PVS = perivitelline space



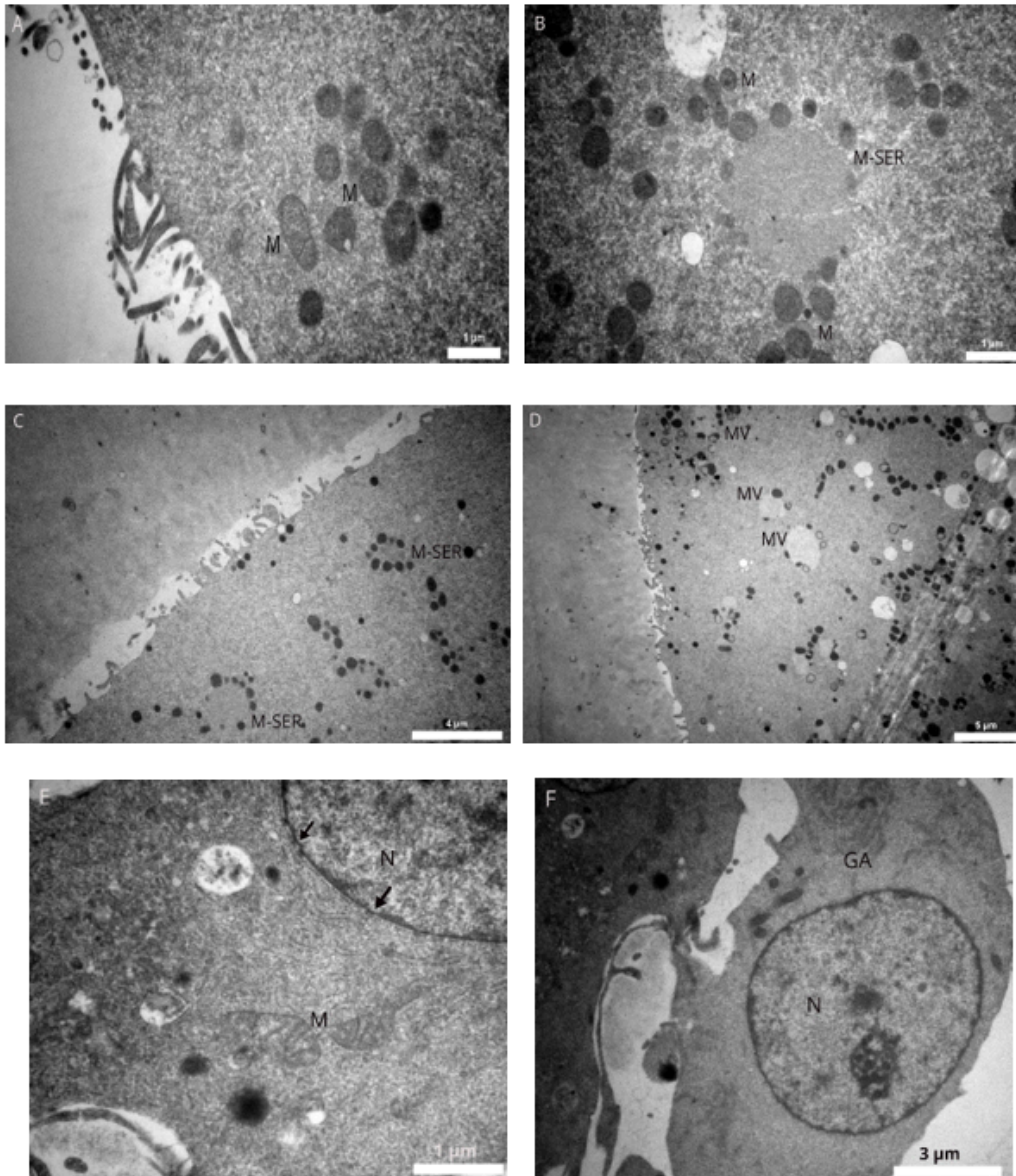


**Figure 5**

General fine structure of MII oocyte and GV oocyte. The round-to-oval mitochondria with a dense matrix and sparse cristae (A). typical mitochondria-smooth endoplasmic reticulum (M-SER) aggregates are visible in in vitro matured oocytes (B, C). Small mitochondria-vesicle (MV) complexes are also observable in (D). Nuclear area of germinal vesicle (GV) oocytes (E). Detail of nuclear envelope with distinct nuclear pores (arrows) (E). Concentration of individual mitochondria in the perinuclear region (E).

The complex structure of GA in immature oocytes (F). M= mitochondria, M-SER= mitochondria-smooth endoplasmic reticulum, MV= mitochondria-vesicle, N= Nuclear, GA = Golgi apparatus